Optimization of conventional spinning process parameters by means of numerical simulation and statistical analysis

Essa, Khamis; Hartley, Peter

DOI:
10.1243/09544054JEM1786

Optimization of conventional spinning process parameters by means of numerical simulation and statistical analysis

K Essa and **P Hartley***
School of Mechanical Engineering, University of Birmingham, Birmingham, UK

The manuscript was received on 20 August 2009 and was accepted after revision for publication on 3 March 2010.

DOI: 10.1243/09544054JEM1786

Abstract: Research in sheet metal spinning has increased due to a greater demand, especially in the transportation industries, for parts with very high strength-to-weight ratios with low cost. Spinning processes are efficient in producing such characteristics and there is great flexibility in the process with a relatively low tool cost. The objectives of this investigation are to define the critical working parameters in spinning, show the effects of these factors on product quality characteristics, and to optimize the working parameters. The example used is the conventional spinning of a cylindrical cup. Optimization of the process is undertaken through the use of statistical analysis tools applied to the data produced from three-dimensional finite element simulations of the process. This has been achieved by generating two 'designs of experiments'. The first identifies the most critical parameters for product formability and the second shows how these critical parameters affect the product quality. The results show that feed rate, relative clearance, and roller nose radius are the most important working parameters and significantly affect average thickness, thickness variation, and springback of the cylindrical cup. An additional 22 per cent improvement in the product quality characteristic is gained through using the optimum working parameters.

Keywords: conventional spinning, finite element modelling, design of experiments, statistical analysis, optimization

1 INTRODUCTION

This work focuses on the conventional spinning process, in particular the production of open-ended cup products in which it is important to maintain a uniform, defect-free wall. In these processes, a circular sheet is clamped between a rotating mandrel and supporting holder. The sheet is gradually shaped over the mandrel through the action of a roller that produces a localized pressure as it moves axially over the outer surface of the sheet to produce a symmetrical product. Since the sheet deformation is imparted incrementally through a localized contact region between the deforming sheet and forming tools, it is important to determine the optimum process conditions in order to provide effective process control to produce high-quality products.

There are a large number of parameters that influence the conventional spinning process which may be described either as machine or workpiece parameters. The machine parameters include rotational mandrel speed, roller feed rate, roller design (e.g. roller nose radius), tool surface quality, and material. The workpiece parameters include sheet thickness, initial blank diameter, and material properties. In addition, there are some common measures, these are the relative clearance between the roller and mandrel, contact pressure, friction coefficient, and sliding velocity [**1**]. It is therefore important to identify the individual parameters and the combination of parameters that most directly affect the process performance.

The conventional spinning of cylindrical aluminium cups has been investigated by El-Khabeery *et al.* [**2**] who analysed the effect of feed rate and

**Corresponding author: School of Mechanical Engineering, University of Birmingham, Edgbaston, Birmingham B15 2TT, UK.*
email: p.hartley@bham.ac.uk

roller nose radius on the wall thickness, cup inner diameter, springback, spinning ratio, surface roughness, and spinning forces. They concluded that as the roller angle and feed rate decrease, most of the measures of spinning quality improve. A large roller nose radius results in large contact between the roller and material which leads to an increase in the resulting forces.

The clearance between the roller and mandrel plays an important role in controlling the deformation during the process. Quigley and Monaghan [**3**] reported that during the conventional spinning process, the distance between the roller and mandrel must be reduced, that is to be less than the sheet thickness, by moving the roller towards the mandrel, to achieve a satisfactory forming operation and avoid geometrical defects. Quigley and Monaghan [**4**] also reported that control of forces could be achieved by keeping a constant distance between the roller and blank in order to limit the force applied to the sheet. This agrees with the results obtained by Zhan *et al.* [**5**], who concluded that the most important factor for controlling the process is the initial roller position in order to avoid any interference between the roller and mandrel in the subsequent spinning process. They also concluded that as the feed rate increases, the force components in the radial, axial, and tangential directions will also increase and the uniformity of the wall thickness will decrease. Such an effect has also been observed by Wong *et al.* [**6**].

Xia *et al.* [**7**] investigated experimentally one-pass spinning of a cylindrical part. In their setup, steel and aluminium blank sheets were formed into a cylindrical cup. Their principal conclusions were:

(a) as feed rate increases, axial force, radial force, and thickness strain increase;
(b) as the relative clearance between the roller and mandrel increases, it has a great impact on increasing the thickness variation;
(c) the speed of the rotating mandrel has no effect on the experimental results.

It was also recorded that when using an initial thickness of more than 1 mm for both aluminium and steel parts, the spinning becomes successful (i.e. no wrinkling or cracking). Similar effects were also recorded by Liu [**8**] who simulated multi-pass and die-less conventional spinning processes using the dynamic explicit LS-DYNA finite element software. Hamilton and Long [**9**] stated that working parameters such as roller feed rate and radius of the round corner of the mandrel have a significant effect on the resulting forces and thickness strain. Wrinkling defects appeared at high values of feed rates.

Bai *et al.* [**10**] studied the springback effect of thin-walled aluminium alloy shell with an inner rib using the ABAQUS/Implicit software. It was reported that the residual stress distribution is more uniform than that before unloading since springback is a stress self-balancing process. The change in one of the product dimensions, the half apex angle, was used to represent the amount of springback. They concluded that the elastic deformation during the process cannot be neglected and it plays an important role in springback effects. They also concluded that the springback effect could be minimized by selecting logical working conditions. Behrouzi *et al.* [**11**] proposed an analytical approach to analyse springback in sheet bending, in which they reported that their model could be applied for various planar bending processes to compensate for the geometric error resulting from springback.

The use of design of experiment (DOE) and statistical analysis, for example, analysis of variance (ANOVA), have been shown to be useful approaches to study the effect of working parameters on sheet metal forming processes. Similar techniques have been used in other processes. For example, Yang *et al.* [**12**] used a Taguchi method to obtain the optimal working parameters in cutting glass fibre, and Bacchewar *et al.* [**13**] used response surface DOE and ANOVA techniques to study the significant process variables in selective laser sintering. Hussain *et al.* [**14**], Ham and Jeswiet [**15**], and Filice *et al.* [**16**] also used similar techniques to investigate the effect of process variables such as feed rate, rotational speed, and sheet thickness on formability in incremental sheet forming. Using two DOEs, Ham and Jeswiet [**17**] assessed the most critical variables for single-point incremental forming in order to get successful deformation, i.e. no tearing or cracking. Then they studied the effect these significant variables had on the process formability. Ambrogio *et al.* [**18**] used statistical analysis methods by means of DOE and ANOVA to obtain an empirical model that related the process variables to the geometrical errors, i.e. springback in incremental forming. Kleiner *et al.* [**19**] used the same approaches to find the optimal working parameters to manufacture high-voltage dividers by shear spinning. They concluded that although the implementation of these statistical methods was easy, an additional improvement of about 20 per cent in process quality was gained.

In this paper a combination of DOE and numerical simulation approaches is used to determine the most important working parameters in conventional spinning and to show how these parameters affect the average thickness, thickness variation, springback, and axial force during the manufacture of a cylindrical cup. Additionally, using a min–max optimization method, the optimum working parameter settings that allow the best quality characteristics to be obtained for this product are determined.

2 NUMERICAL MODELS OF CONVENTIONAL SPINNING PROCESS

All the models presented in this paper were developed using ABAQUS/Explicit v6.8. Conventional spinning involves the forming of a circular sheet which is clamped between a rotating mandrel and supporting holder. The sheet is gradually shaped over this rotating mandrel through the action of a roller that produces a localized pressure and moves axially over the outer surface of the sheet. In the example here the mandrel had a diameter of 118 mm and rotated with a constant rotational speed of 200 rpm. An aluminium sheet blank with an original diameter of 192 mm and thickness of 3 mm was attached to the mandrel. The holder had a diameter of 112 mm [**7**, **9**]. The validity of the finite element models used here has been established by [**20**] who compared simulation results for axial force, radial force, and strain to the experimental data of Xia *et al.* [**7**]. At the beginning of the finite-element (FE) simulation, the holder pushed the sheet forward to the mandrel with a small constant load of 100 kN in order to keep the sheet secure between the mandrel and the holder. Thus, the sheet and holder rotate with the same mandrel speed. These details are shown in Fig. 1.

The mandrel, holder, and roller were modelled as rigid bodies, whereas the sheet was modelled as an elastic–plastic deformable body using the material properties of pure aluminium (A-1100-O). The stress–strain curve for this aluminium is described by $\sigma = 148\varepsilon^{0.233}$, with an initial yield stress of 100 MPa and a mass density of 2700 kg/m^3. Isotropic elasticity was assumed with a Young's modulus of 70 GPa and a Poisson ratio of 0.3. The material data were taken from Long and Hamilton [**21**], originally presented in Kalpakjian and Schmid [**22**]. While recognizing the importance of thermal and rate effects, and of anisotropy in sheet forming processes, these effects are not included in the present model as the objective is to assess the use of statistical methods combined with FE modelling. Coulomb friction was set with a friction coefficient of 0.2, 0.5, and 0.05 between the sheet and the mandrel, holder, and roller respectively as assumed in [**9**, **21**].

In the FE model used here the mass inertia of the roller was defined so that the roller can rotate about its axis when contacting the sheet. Three-dimensional (3D) eight-node linear hexahedral elements were used to mesh the sheet. The number of elements in the thickness direction was two, this was the minimum number of elements required to properly reproduce the bending deformation around the mandrel corner without excessive element distortion [**20**]. The total number of elements was 5968, with 9102 nodal points. Figure 2 shows the FE model and arrangement of components for the single-pass conventional spinning process. All simulations were performed on an Intel® CoreTM Dual computer with a 3 GHz CPU. Several values of load rate scaling were applied to reduce the simulation time. A maximum scaling factor of 21 was used, which provided a significant reduction in simulation time while maintaining a similar accuracy in the numerical results [**20**].

An assessment of the stability of the numerical solution was undertaken in [**20**] to ensure that the solution was close to quasi-static conditions, and also a comparison of the results to experimental data was performed. Figure 3 shows an example of the progressive state of deformation and von Mises' stress distribution for this case. It can be seen that for a roller displacement of less than 20 mm, where there is no contact between the deforming sheet and the sides of the mandrel, the deformation state is essentially free bending. For roller displacements of between 20 and 40 mm, the geometry developed during deformation closely resembles that in deep drawing. For roller displacements of more than 40 mm, the deformation state is a combination of compression and bending,

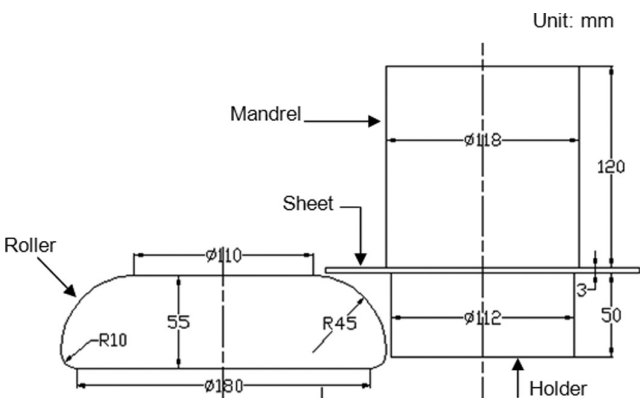

Fig. 1 Geometries and dimensions of the model [**9**]

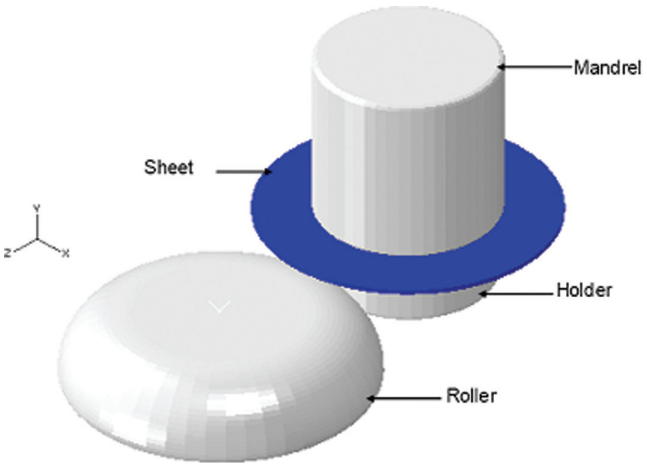

Fig. 2 FE model of conventional spinning process [**20**]

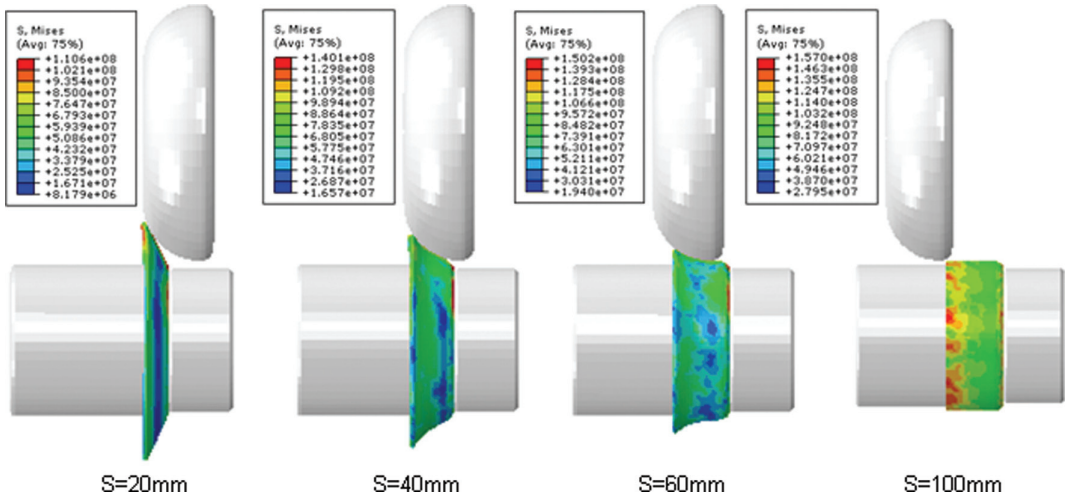

Fig. 3 Deformation states during single-pass conventional spinning, S is the linear, axial displacement of the roller [**20**]

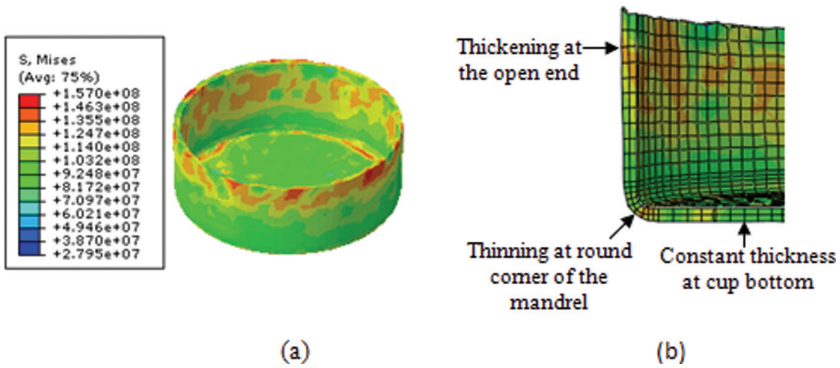

Fig. 4 (a) Von Mises stress in the fully deformed cup and (b) a section through the cup with the FE mesh superimposed revealing the local thinning [**20**]

where the sheet is compressed between the roller and mandrel which occurs simultaneously with the bending deformation around the mandrel corner [**20**]. Figure 4(a) shows the shape of the fully deformed cup and Fig. 4(b) shows a cross-section indicating the thickness distribution of the final cup. Local thinning in the corner region is evident.

The distribution of von Mises stress shown in Fig. 4(a) reveals a reasonably uniform level for much of the deformed wall of the cup, but with some variations, especially on the inner surface of the wall, towards the open end. Figure 4(b) shows a typical distribution of wall thickness variations in which the base of the cup which was held between the mandrel and holder is almost constant, while there is local thinning around the mandrel corner and slight thickening near the open end. Additionally, no wrinkling can be observed for the shown example [**20**].

In this study, two DOEs were conducted. For the first DOE, process parameters were included and the objective of this DOE was to define the most critical forming parameters in conventional spinning. The response for the first DOE is a qualitative measurement (either good, i.e. formed without defects, or a failed part). The objective of the second DOE is to show the effect of critical working parameters only on some of the process quality characteristics. The combination of the first DOE and the second DOE gives a comprehensive, in-depth analysis of the conventional spinning process and minimizes the number of terms that will be used in the prediction of selected process quality characteristics.

3 THE FIRST DOE

A selection DOE has not been used in previous investigations [**2**, **7**–**10**, **21**] which would have provided a set of guidelines providing justification for the chosen critical parameters. Based on the use of a selection DOE, a Box–Behnken design was used to generate a set of experiments for six process factors with each factor being varied over three levels, high level, intermediate level, and low level.

3.1 Description of factors, levels, and response variable

In conventional spinning processes, the factors that affect the product quality are feed rate, mandrel rotational speed, relative clearance between the roller and mandrel, friction coefficient, roller nose radius, sheet thickness, and initial blank diameter. All these process parameters were considered in the first DOE. The levels of feed rate, relative clearance between the roller and mandrel, sheet thickness, and initial blank diameters were taken from the experimental investigation by Xia *et al.* [**7**]. In most previous investigations, the mandrel rotational speed has been 200 rpm, whereas in the current study it was varied between 100 and 300 rpm, which provides a logical range. The roller nose radius normally used has been 10 mm whereas in this study, a further two levels of 15 and 20 mm were added. Finally, the previous published FE models used a friction coefficient of 0.05, a further two levels of zero (no friction) and at 0.1 (high friction) were used in this work. Table 1 shows the different process factors and the corresponding levels.

The response variables are the quality characteristics (QCs), which generally refer to the measured results. The QC can be a single criterion (quantitative) such as pressure, temperature, efficiency, hardness, surface finish, etc. or combination of several criteria together in a single index. QC also refers to the nature of the performance objectives (qualitative) such as 'bigger is better' or 'smaller is better'. For the first DOE, a qualitative response, 'amplitude of wrinkling or severe thinning' was used to represent the forming quality or formability of the products. An index for different levels of the amplitude of wrinkling or severe thinning is shown in Table 2.

Table 1 Process factors and corresponding levels

	Level		
Factor	Low	Intermediate	High
Roller feed rate (mm/rev)	0.5	2.75	5.0
Mandrel revolution (rpm)	100	200	300
Relative clearance (%)	−20	0	20
Friction coefficient	0	0.05	0.1
Roller nose radius (mm)	10	15	20
Sheet thickness (mm)	1	2	3
Initial blank diameter (mm)	192	198	204

Table 2 An index for the different levels of qualitative response

	Category		
Response	0	1	2
Amplitude of wrinkling or severe thinning	None	Intermediate	Strong

The result of running the first Box–Behnken design was a table showing the order of implementation of the 62 experiments, which present different combinations of the previous factor levels. These combinations were assessed through the use of a 3D FE model of the forming of a cylindrical cup by the conventional spinning process using the ABAQUS/Explicit code. For each combination, an index for the amplitude of wrinkling or severe thinning was given. Typical results are shown in Fig. 5.

3.2 First DOE results

Based on the main effect model, the relationships between the process variables and response variable were estimated. The ANOVA method was used to identify the most important factors. Values of the R-square and adjusted R-square, a measure of model fit, showed that each of the models described the relationship between the factors and the quality characteristic reasonably, these were 92 and 90 per cent respectively. The results of the first DOE are presented in Table 3 and are shown in a standard factor plot (response diagram) in Fig. 6.

The factor plot shows feed rate, relative clearance, roller nose radius, and sheet thickness all have a critical effect on product formability (ability of forming without wrinkling or severe thinning). Initial diameter is more likely to enhance the formability when the values are low. Mandrel rotational speed and coefficient of friction did not show any effect on the formability.

Using too low or too high axial feed rates leads to wrinkling defects. Using a too low feed rate allows the material to flow in the outer direction and using a too high axial feed rate causes excessive stresses in the radial and circumferential directions that lead to radial and circumferential cracking [**23**]. Accordingly, both results lead to wrinkling and severe thinning. Therefore, an optimum value of axial feed rate should be used to avoid this kind of defect.

The relative clearance between the roller and mandrel clearly plays an important role in the conventional spinning process. When using a relative clearance with a negative value, the distance between the roller and mandrel becomes less than the initial thickness which causes a thickness reduction. As this negative value increases, the volume of the material to be reduced increases causing the material to build up in front of the roller. As a result, a large amplitude of wrinkling can be observed. Using a high positive relative clearance value tends to reduce the rigid contact between the roller and the sheet and allows the material to escape from beneath the roller causing dimensional and geometrical inaccuracy. Therefore, an optimum value for axial feed rate and relative clearance between the roller and mandrel

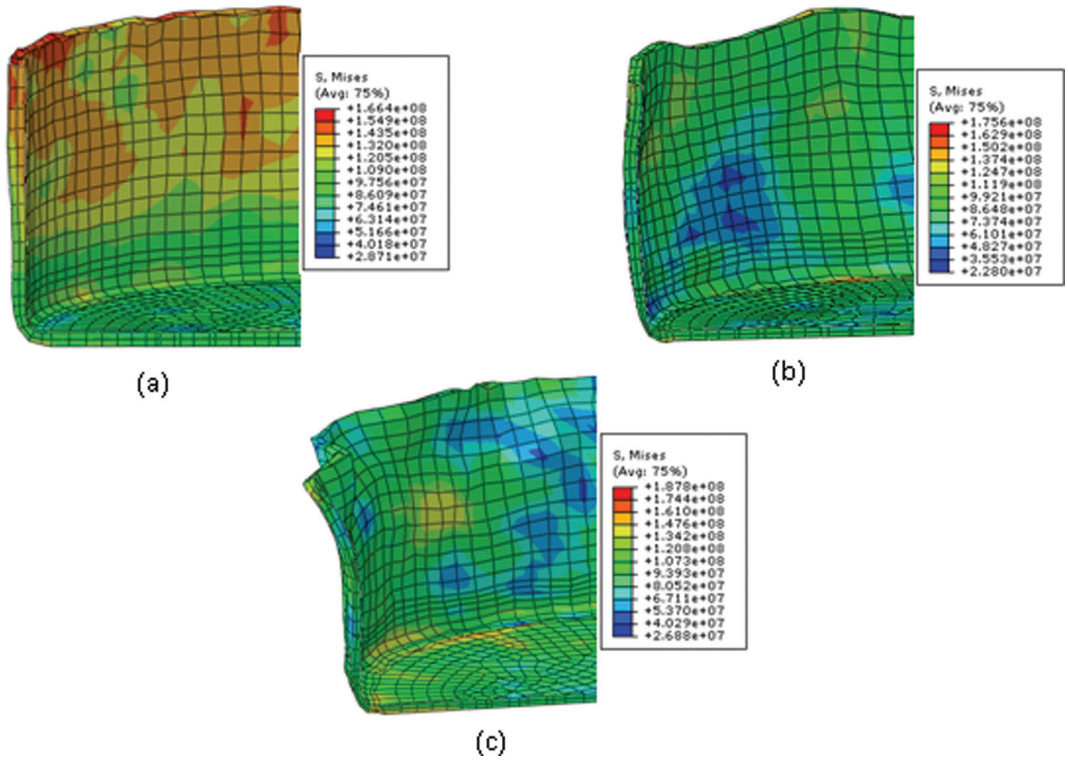

Fig. 5 Typical results of wrinkling and severe thinning in the first DOE (a) none (index 0), (b) intermediate (index 1), and (c) strong (index 2)

should be selected in order to obtain defect-free products.

After the state of free bending deformation at the beginning of the process, the roller nose radius is completely responsible for the rest of the deformation states. Using a large roller nose radius leads to an increase in the contact area between the roller and the sheet which provides greater forming stability [**24**]. However, this naturally leads to a decrease in the contact pressure of the roller and the generated stresses including the compressive tangential stress component will decrease [**1**]. On the other hand, it is known that compressive tangential stress will compensate the thinning caused by tensile radial stresses. Therefore, a too large roller nose radius is found to increase the severe thinning which is a result of the unfavourable large contact area between the roller and the sheet.

Sheet thickness plays a very important role in the process formability. It is known that the maximum axial force corresponds to the maximum plastic deformation that takes place near the round corner of the mandrel (cup bottom) [**7**]. After that, the force decreases as necking occurs at the corner of the mandrel under large axial tensile stresses. If the sheet thickness is unable to support these large axial tensile stresses, circumferential cracking and fracture at the cup bottom are expected [**7**]. The results obtained agree with this, where only one cup is formed successfully for 1 mm sheet thickness and five for 2 mm sheet thickness. Both results show a low formability index when compared to the 20 cups formed successfully for 3 mm sheet thickness.

In conventional spinning, the drawing ratio, m, is a relationship between the initial blank diameter, mandrel diameter, and initial thickness as shown in equation (1) [**7**]. For fixed sheet thickness and mandrel diameter, as the initial blank diameter increases, the nominal drawing ratio will be increased as shown in equation (1). When cups are spun with a large drawing ratio, large tensile forces are created and hence lead to an increase in the tensile stress. This results in a decrease in sheet thickness and large thinning can be observed at the cup bottom. Consequently, for the second DOE, the sheet thickness and initial blank diameter were fixed at 3 and 192 mm respectively in order to avoid having defective parts and to optimize the process at fixed product dimensions.

$$m = D_s/(D_m + t_o) \tag{1}$$

where m is the drawing ratio, D_s is the initial sheet diameter, D_m is the mandrel diameter, and t_o is the sheet thickness. The mandrel rotational speed and friction coefficient do not appear to influence the process formability. This agrees with the observations of previous investigations. Xia *et al.* [**7**] concluded

Table 3 First DOE results for wrinkling and severe thinning

Run	Feed rate (mm/rev)	Mandrel speed (rpm)	Relative clearance (%)	Friction coefficient	Roller nose radius (mm)	Sheet thickness (mm)	Initial blank diameter (mm)	Amplitude of wrinkling and severe thinning
1	0.5	200	−20	0.05	10	2	198	2
2	2.75	200	0	0.05	15	2	198	0
3	2.75	100	0	0.05	10	2	204	1
4	2.75	200	0	0	20	3	198	0
5	2.75	300	20	0.05	15	1	198	2
6	5	100	0	0	15	2	198	1
7	2.75	200	0	0.1	20	3	198	0
8	5	300	0	0.1	15	2	198	2
9	2.75	100	0	0.05	20	2	192	0
10	2.75	200	0	0.05	15	2	198	0
11	0.5	100	0	0.1	15	2	198	2
12	0.5	300	0	0	15	2	198	1
13	0.5	100	0	0	15	2	198	1
14	0.5	200	0	0.05	15	3	204	0
15	2.75	300	0	0.05	10	2	204	2
16	0.5	200	0	0.05	15	1	192	1
17	2.75	100	20	0.05	15	1	198	1
18	2.75	200	0	0	10	3	198	0
19	2.75	200	0	0.05	15	2	198	0
20	0.5	200	0	0.05	15	3	192	0
21	5	100	0	0.1	15	2	198	2
22	2.75	200	20	0	15	2	192	0
23	0.5	200	20	0.05	20	2	198	2
24	5	300	0	0	15	2	198	2
25	2.75	100	−20	0.05	15	1	198	1
26	2.75	200	0	0.1	20	1	198	2
27	2.75	200	0	0.1	10	3	198	0
28	2.75	200	20	0	15	2	204	0
29	2.75	300	0	0.05	20	2	204	2
30	5	200	0	0.05	15	3	192	0
31	2.75	200	20	0.1	15	2	204	1
32	2.75	200	0	0.1	10	1	198	1
33	5	200	20	0.05	20	2	198	0
34	2.75	200	0	0.05	15	2	198	0
35	5	200	0	0.05	15	3	204	0
36	2.75	200	0	0	10	1	198	2
37	2.75	200	0	0	20	1	198	1
38	0.5	200	−20	0.05	20	2	198	2
39	2.75	200	0	0.05	15	2	198	0
40	0.5	200	0	0.05	15	1	204	1
41	2.75	100	20	0.05	15	3	198	0
42	2.75	200	0	0.05	15	2	198	0
43	2.75	300	−20	0.05	15	3	198	0
44	5	200	−20	0.05	10	2	198	2
45	2.75	300	20	0.05	15	3	198	0
46	5	200	0	0.05	15	1	192	2
47	2.75	100	0	0.05	10	2	192	0
48	2.75	200	20	0.1	15	2	192	0
49	2.75	100	0	0.05	20	2	204	1
50	2.75	200	−20	0.1	15	2	204	0
51	2.75	300	−20	0.05	15	1	198	2
52	5	200	−20	0.05	20	2	198	1
53	0.5	300	0	0.1	15	2	198	2
54	5	200	0	0.05	15	1	204	2
55	2.75	100	−20	0.05	15	3	198	0
56	2.75	200	−20	0.1	15	2	192	1
57	5	200	20	0.05	10	2	198	1
58	0.5	200	20	0.05	10	2	198	2
59	2.75	200	−20	0	15	2	204	1
60	2.75	300	0	0.05	10	2	192	0
61	2.75	200	−20	0	15	2	192	0
62	2.75	300	0	0.05	20	2	192	0

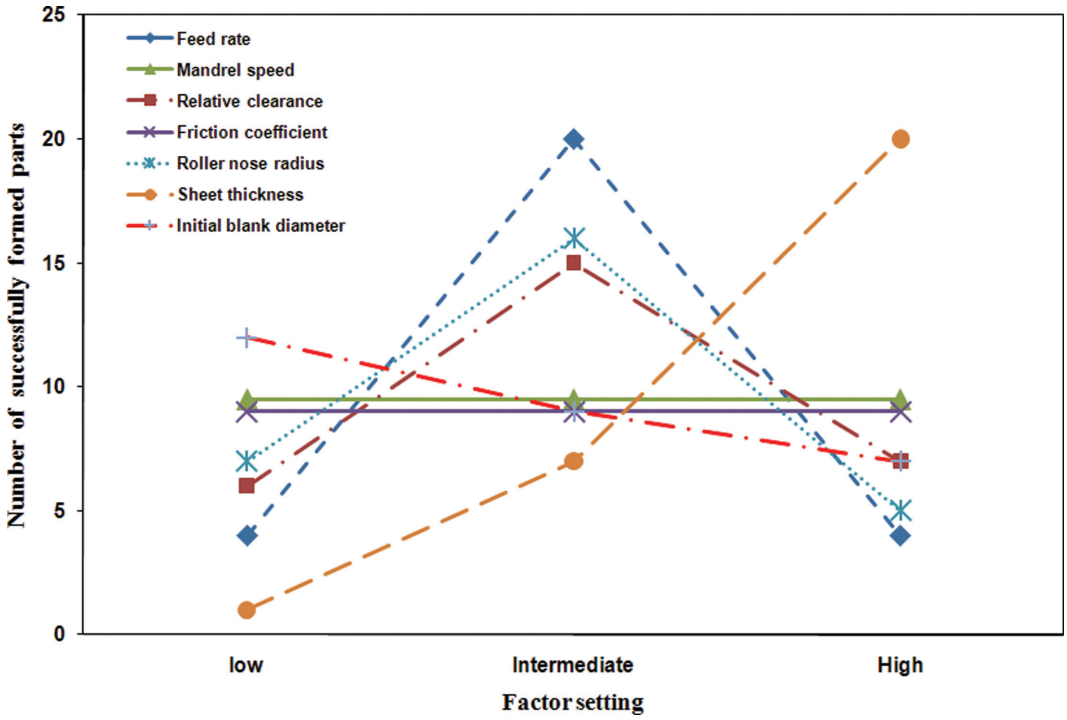

Fig. 6 Factor comparison of working parameters used in the first DOE

that mandrel rotational speed has no appreciable effect on the experimental results. Additionally, the friction coefficient did not show any effect on the results in previous FE models [**8**, **9**, **21**].

4 THE SECOND DOE

The objectives of the second DOE were to show the effect of feed rate, relative clearance, and roller nose radius on the average thickness, thickness variation, springback, and axial force. Additionally, to obtain an empirical model that can predict these responses for any combination of the working parameters. This will help to optimize the working parameters and obtain a final product with high quality. Box–Behnken design was used to generate a set of experiments for only these three factors.

4.1 Description of factors, levels, and response variable

Each of the selected factors for the second DOE was varied over three levels as shown in Table 4. The levels of these factors are exactly the same as for the first DOE. The mandrel rotational speed, friction coefficient, sheet thickness, and initial blank diameter were kept constant at 200 rpm, 0.05, 3 mm, and 192 mm respectively. As previously mentioned, the rotational mandrel speed and friction coefficient have no critical effect. On the other hand, sheet thickness and initial blank diameter were kept fixed at 3 and 192 mm respectively to avoid having defective parts and to optimize the process for specified product dimensions.

Table 4 Process factors and corresponding levels

	Level		
Factor	Low	Intermediate	High
Roller feed rate (mm/rev)	0.5	2.75	5.0
Relative clearance (%)	−20	0	20
Roller nose radius (mm)	10	15	20

In the second DOE, the QCs were selected to represent the product quality that involves only qualitative measurements. Quantitative QCs include average thickness, thickness variation, diameter springback, and maximum axial force. For each experiment, the thickness was measured at eight points along the depth of cup, and the average thickness and standard deviation were then calculated. Standard deviation was used to indicate the thickness variation. The final inner diameter of the cup was also measured at eight different points and the maximum deviation from the mandrel diameter was used to indicate the springback. Finally, the maximum value for the axial force was recorded for each combination.

The result of running the second Box–Behnken design was a table showing the order of implementation of the 17 experiments, which present different

Table 5 QCs for the 17 experiments

Run	Feed rate (mm/rev)	Relative clearance (%)	Roller nose radius (mm)	Average thickness (mm)	Thickness variation (mm)	Springback (mm)	Maximum axial force (N)
1	2.75	0	15	2.95	0.46	0.75	3153
2	2.75	−20	20	2.59	0.19	1.40	3716
3	0.50	−20	15	2.49	0.24	0.53	2499
4	2.75	20	20	3.04	0.58	0.80	3219
5	2.75	20	10	3.10	0.53	0.71	2861
6	5.00	20	15	3.08	0.54	1.11	3103
7	5.00	−20	15	2.74	0.33	2.06	3382
8	2.75	0	15	2.95	0.46	0.75	3153
9	2.75	0	15	2.95	0.46	0.75	3153
10	0.50	20	15	2.92	0.37	0.50	2179
11	2.75	0	15	2.95	0.46	0.75	3153
12	5.00	0	20	2.95	0.40	1.34	3748
13	2.75	−20	10	2.54	0.19	1.31	2933
14	0.50	0	10	2.86	0.28	0.44	2172
15	5.00	0	10	3.02	0.43	1.36	2912
16	2.75	0	15	2.95	0.46	0.75	3153
17	0.50	0	20	2.74	0.35	0.52	2589

combinations of the previous factor levels as shown in Table 5. These combinations were used in the 3D FE simulation of the formation of a cylindrical cup by the conventional spinning process.

4.2 Second DOE results

Table 5 shows the numerical results for the average thickness, thickness variation, springback, and maximum axial force for 17 experiments. An ANOVA was performed on the DOE to identify the significant factors and interactions. A significance level of 5 per cent was used. In statistical hypothesis testing, the P-value is the probability of obtaining a result at least as good as the one that was actually observed, assuming that the null hypothesis is true [**25**]. The fact that P-values are based on this assumption is crucial to their correct interpretation. The smaller the P-value (less than 5 per cent) the more important the factor. Table 6 shows the P-values for the significant factors and interactions. According to the value of R-square and adjusted R-square, the Box–Behnken statistical analysis highlights that a quadratic model provides a very good description of the QCs evolution with respect to the working parameters. The R-square and adjusted R-square values for all responses did not go below 95 per cent.

The ANOVA study shows that feed rate affects average thickness, thickness variation, springback, and maximum axial force. Relative clearance affects average thickness, thickness variation, and maximum axial force. Roller nose radius only affects the maximum axial force. The interactions between feed rate and relative clearance, relative clearance and roller nose radius affect the maximum axial force. It is important to note that no defective products are observed and only very weak wrinkling is recognized for run numbers 3 and 7. This is a result of using a very high or very low feed rate with a large negative relative clearance.

Table 6 Significant factors and corresponding P-values

	Average thickness	Thickness variations	Springback	Maximum axial force
Feed rate (A)	0.002	0.016	0.001	0.001
Relative clearance (B)	0.001	0.001	0.132	0.001
Roller nose radius (C)	0.123	0.481	0.869	0.001
Significant interactions				($A \times B$) 0.001 ($B \times C$) 0.001

4.3 Average thickness

Figure 7(a) shows the effect of feed rate on the average thickness. Using a high feed rate leads to an increase in the compressive tangential stress and accordingly, compressive deformation and thickness strain increase. The final average thickness will therefore deviate away from the initial thickness. This agrees with results obtained by El-Khabeery *et al.* [**2**]. Figure 7(b) shows the effect of relative clearance on the average thickness. It can be seen that the effect of relative clearance on the average thickness is more obvious. This is due to the fact that as relative clearance decreases (using a large negative value) extensive sheet thinning in the thickness direction takes place. However, decreasing the relative clearance between the roller and sheet results in a more uniform thickness distribution as will be shown later. This was also observed by Xia *et al.* [**7**]. Therefore, the relative clearance needs to be carefully selected.

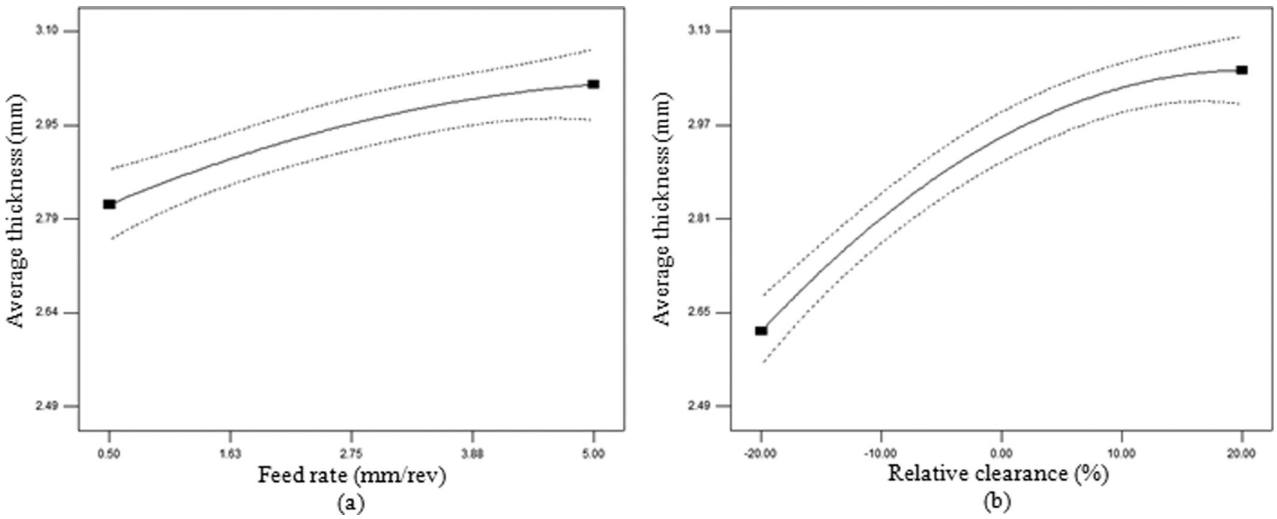

Fig. 7 Effect of (a) feed rate, and (b) relative clearance on the average thickness

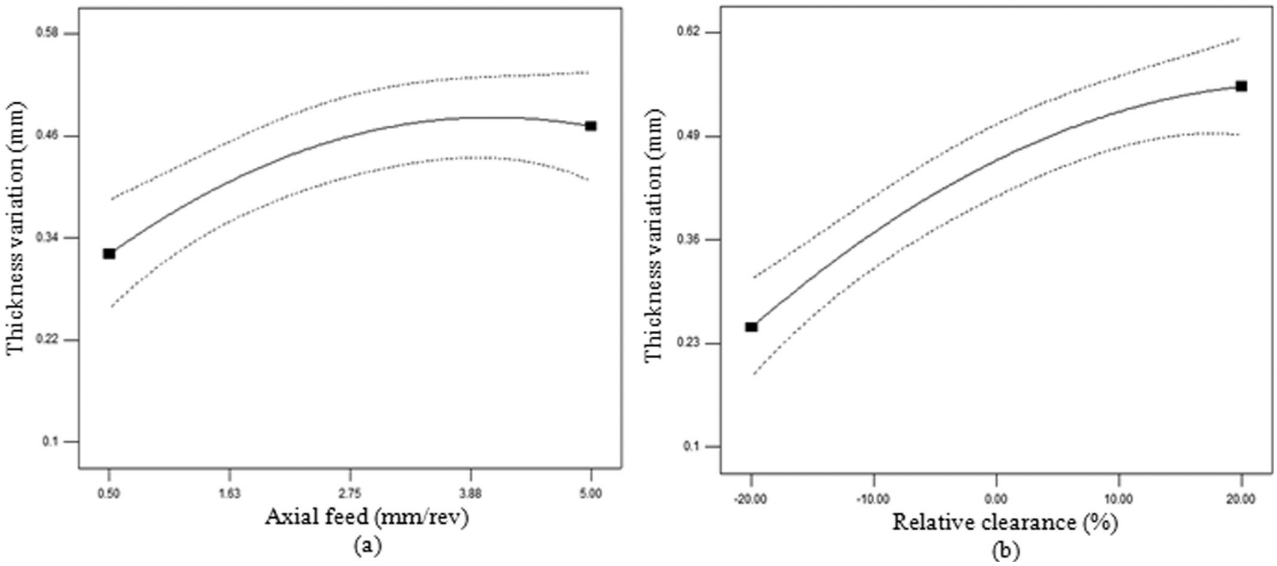

Fig. 8 Effect of (a) feed rate, and (b) relative clearance on the thickness variation

4.4 Thickness variation

Figures 8(a) and (b) show the effect of feed rate and relative clearance on the thickness variation. It can be seen that both have the same effect. In order to obtain a more uniform thickness distribution, a low feed rate and a negative relative clearance should be used. High feed rates increase the contact area between the roller and workpiece that tends to decrease the applied stresses [**2**]. Therefore, the workpiece deformation decreases and thus, a high thickness variation is found. By decreasing the relative clearance, additional plastic deformation is induced which results in the material work hardening, increasing and restricting any further thinning of the formed part. Accordingly, the differences between the earlier and later deformation decrease and thus, the thickness distribution becomes more uniform.

4.5 Springback

Figure 9 shows the effect of feed rate on the springback. As shown, increasing the axial feed rate has a significant impact on increasing springback and an increase in inner diameter at the open end is found. It is known that a low feed rate is usually accompanied by an over-rolling between the roller and sheet material as suggested by El-Khabeery *et al.* [**2**] which leads to an increase in temperature in the deformation zone. This affects the material elasticity significantly and reduces the material recovery. El-Khabeery *et al.* [**2**] reported that at a high feed rate this over-rolling does not occur and the generated

temperatures are lower than that at a low feed rate. Therefore, after removing the roller, springback will occur which leads to an increase in the inner diameter and bulging of the final cup. It is important to note that the maximum diameter opening takes place near to the middle of the cup depth, which also agrees with the previous results obtained by El-Khabeery *et al.* [**2**].

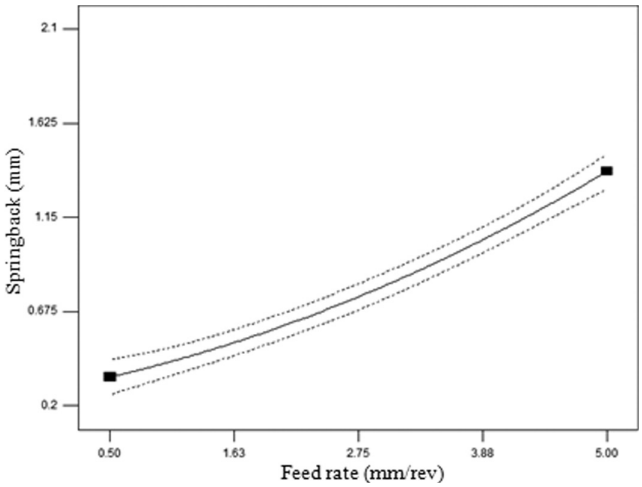

Fig. 9 Effect of feed rate on the springback

4.6 Maximum axial force

In the conventional spinning processes, the axial force is the main forming force. Figure 10(a) shows the effect of feed rate on the axial force. As the axial feed rate increases, the maximum axial force increases. An increasing axial feed rate leads to an increase in the volume of material underneath the roller per unit time. Hence, a higher deformation power is required, therefore, an increase in the maximum axial force is observed. Figure 10(b) shows the effect of relative clearance on the maximum axial force. It shows that the maximum axial force increases with a decrease in the relative clearance. Consequently, a large thinning in the sheet thickness occurs and thus, the spinning forces increase. Figure 10(c) shows that as the roller nose radius increases, the maximum axial

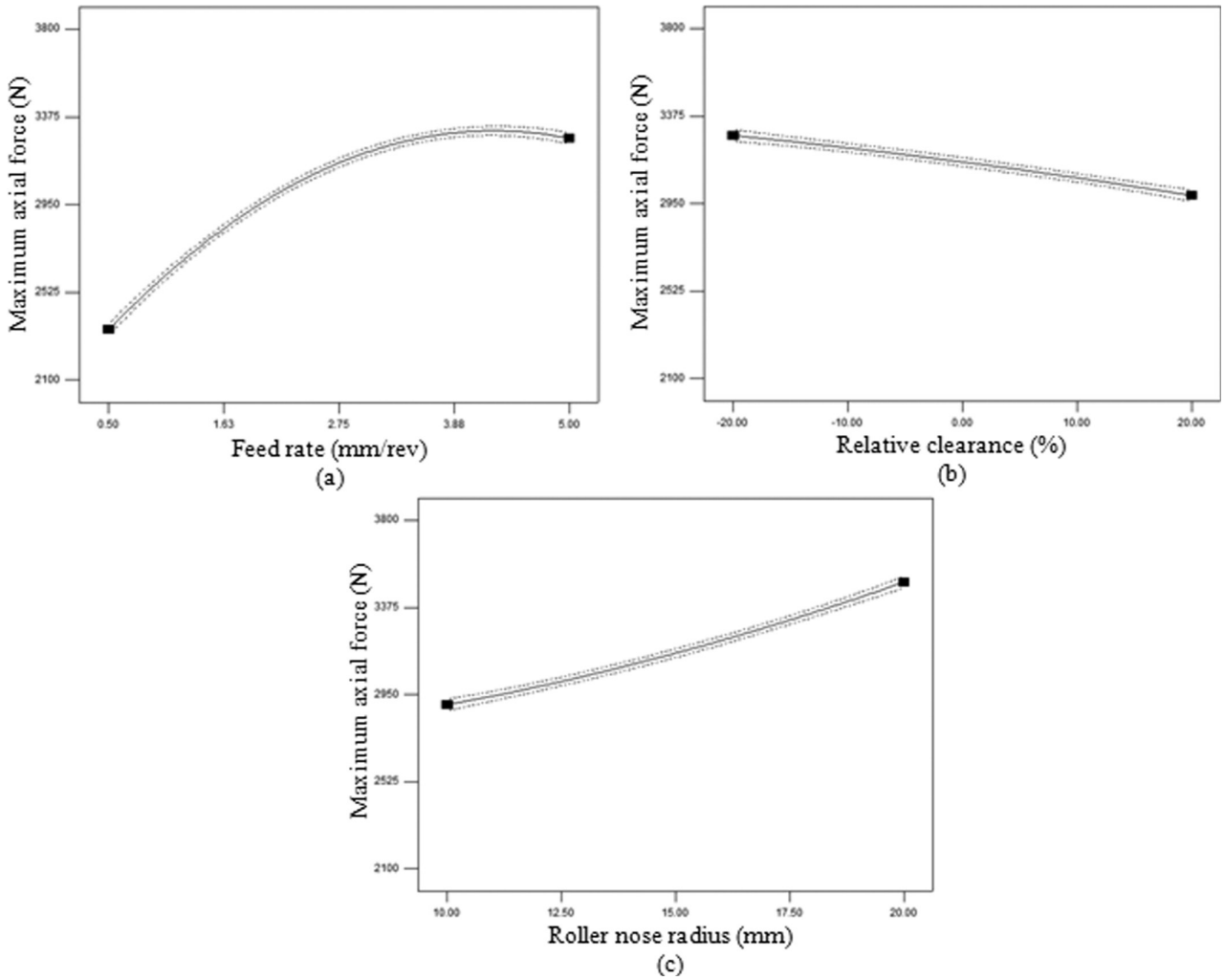

Fig. 10 Effect of (a) feed rate, (b) relative clearance, and (c) roller nose radius on the maximum axial force

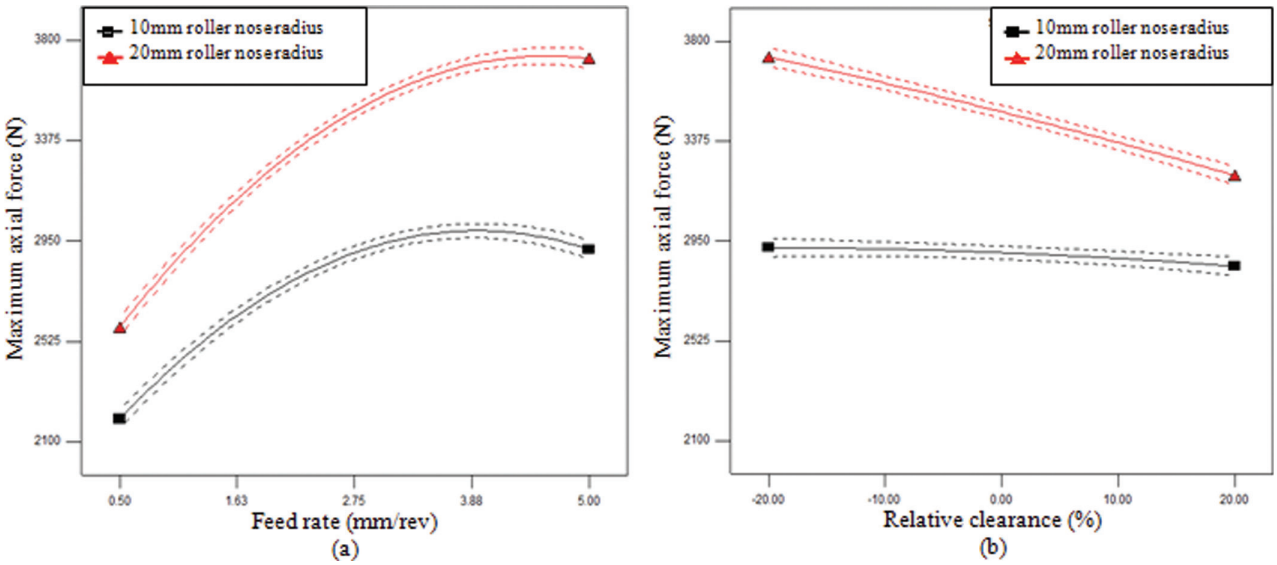

Fig. 11 Effect of interactions between (a) feed rate and roller nose radius, and (b) relative clearance and roller nose radius on the maximum axial force

force increases. It is clear that as roller nose radius increases, the contact area between the roller and sheet material also increases. Hence, the power, and the axial force, required to produce the cup, will be larger.

Figures 11(a) and (b) show the effect of the interactions between feed rate and roller nose radius, relative clearance and roller nose radius on the maximum axial force respectively. A high feed rate and large roller nose radius increase the maximum axial force significantly as shown in Fig. 11(a). The large amount of material to be formed and large contact area that resulted from using high values of both factors lead to an increase in the required deformation power and thus, the axial force increases. With a small roller nose radius, the relative clearance has no influence on the axial force. Since the roller nose radius increases and a negative relative clearance was used, the deformation power increases and axial force increases. This is due to an increase in the contact area between the roller and sheet material resulting from using a large roller nose radius in addition to a significant thickness reduction resulting from the use of a negative relative clearance.

5 PREDICTION OF EACH QC

It is useful to develop an empirical model that allows the description and prediction of each of the selected QCs under any combination of process parameters. As a result of using numerical factors in this study, it is possible to predict the equivalent QCs at any value of each process parameter even if it was not one of the preselected levels. Using a general second-order polynomial equation, an empirical model is constructed based on the critical parameters, i.e. feed rate, relative clearance, and roller nose radius and their interactions. Each process parameter and interaction is multiplied by a coefficient as shown in equation (2). The value of each coefficient under each quality characteristic is displayed in Table 7. R-square for all models did not go below 95 per cent.

$$\text{Quality characteristic} = X + x_1A + x_2B + x_3C + x_4AB + x_5AC + x_6BC + x_7A^2 + x_8B^2 + x_9C^2 \quad (2)$$

where A is the feed rate, B is the relative clearance between the roller and mandrel, C is the roller nose radius and x_1–x_9 are the model coefficients indicated in Table 7.

6 OPTIMIZATION OF WORKING PROCESS PARAMETERS

In order to obtain a spun product with high dimensional accuracy and high surface quality, the optimal working conditions need to be selected. In this study, the objective function is to obtain a final product that has a thickness close to 3 mm, minimum thickness variation, minimum springback, and zero amplitude of wrinkling or severe thinning. Since there are no observed defective parts at the 3 mm sheet thickness, the last objective function was excluded. The objective function for the maximum axial force was ignored when it did not represent any dimensional or surface quality. All process parameters

Table 7 Coefficient values corresponding to each QC

	Average thickness (mm)	Thickness variation (mm)	Springback (mm)	Maximum axial force (N)
Constant (X)	2.688×10^{0}	-1.336×10^{-1}	1.027×10^{0}	1.980×10^{3}
x_1	6.333×10^{-2}	1.359×10^{-1}	2.303×10^{-1}	4.406×10^{2}
x_2	1.663×10^{-2}	6.729×10^{-3}	4.306×10^{-4}	8.011×10^{0}
x_3	2.044×10^{-2}	4.586×10^{-2}	-1.206×10^{-1}	-2.201×10^{1}
x_4	-5.000×10^{-4}	-3.333×10^{-4}	-5.111×10^{-3}	2.278×10^{-1}
x_5	1.111×10^{-3}	-2.222×10^{-3}	-8.222×10^{-3}	9.311×10^{0}
x_6	-2.750×10^{-4}	1.250×10^{-4}	7.286×10^{-19}	-1.063×10^{0}
x_7	-6.667×10^{-3}	-1.259×10^{-2}	2.247×10^{-2}	-6.807×10^{1}
x_8	-2.719×10^{-4}	-1.531×10^{-4}	4.656×10^{-4}	-4.406×10^{-2}
x_9	-9.500×10^{-4}	-1.250×10^{-3}	4.750×10^{-3}	1.875×10^{0}

Table 8 Optimal working parameters

	Axial feed (mm/rev)	Relative clearance (%)	Roller nose radius (mm)
Optimal condition	0.62	−7.33	10

Table 9 Predicted and observed QCs at the optimal working parameters

	Average thickness (mm)	Thickness variation (mm)	Springback (mm)	Maximum axial force (N)
Predicted	2.73	0.20	0.44	2266
Observed	2.74	0.22	0.46	2204

were constrained within their preselected levels and all quality characteristics given the same weight. Using a min–max optimization method, the optimum working parameters that achieve all the objective functions were obtained and they are shown in Table 8. This was achieved by solving the three empirical equations of average thickness, thickness variation, and springback together until the values of working variables that met all objective functions (i.e. 3 mm thickness, minimum thickness variation, and minimum springback) were found.

To validate this approach, a single experiment using the optimal working parameters was performed using the same 3D FE model. All the QCs were measured and compared to those predicted by the model as shown in Table 9. No amplitude of wrinkling or severe thinning was observed. The desirability function, a function that shows how the different QCs results meet all the required objective functions is applied for all experimental runs and the optimal condition. For the spun components of the second Box–Behnken design, overall desirabilities between 0 and 66 per cent were observed. For the optimal working setting, an overall desirability of 88 per cent was observed as shown in Fig. 12. Hence, compared to the best spun component from the 17 experiments, an additional improvement of more than 22 per cent could be gained as shown in Fig. 12. It is important to note that the obtained working parameters are valid only under the preselected sheet dimensions. However, for different sheet dimensions, only the last 17 experiments are required to be conducted using these new dimensions rather than the whole procedure.

7 CONCLUSIONS

1. Using the DOE approach, an experimental plan was generated and conducted through numerical simulation of the spinning process. The results were assessed using the ANOVA technique to identify the most critical working parameters.
2. It was observed that the feed rate, relative clearance between the roller and mandrel, roller nose radius, and sheet thickness were the most critical variables affecting the process formability, i.e. ability of forming without wrinkling or severe thinning. The initial sheet diameter, whilst important, had less effect. The rotational mandrel speed and friction coefficient had no observable effect upon the process formability.
3. For each of the responses, i.e. average thickness, thickness variation, springback, and maximum axial force, significant parameter interactions were identified and a mathematical model was fitted which described the influence of the machine factors reasonably well.
4. As feed rate increased, the average thickness, thickness variation, springback, and maximum axial force increased. A negative relative clearance decreased the average thickness, reduced the thickness variation, and increased the maximum axial force. A large roller nose radius resulted in a large contact between the roller and sheet material which led to an increase in the maximum axial force.

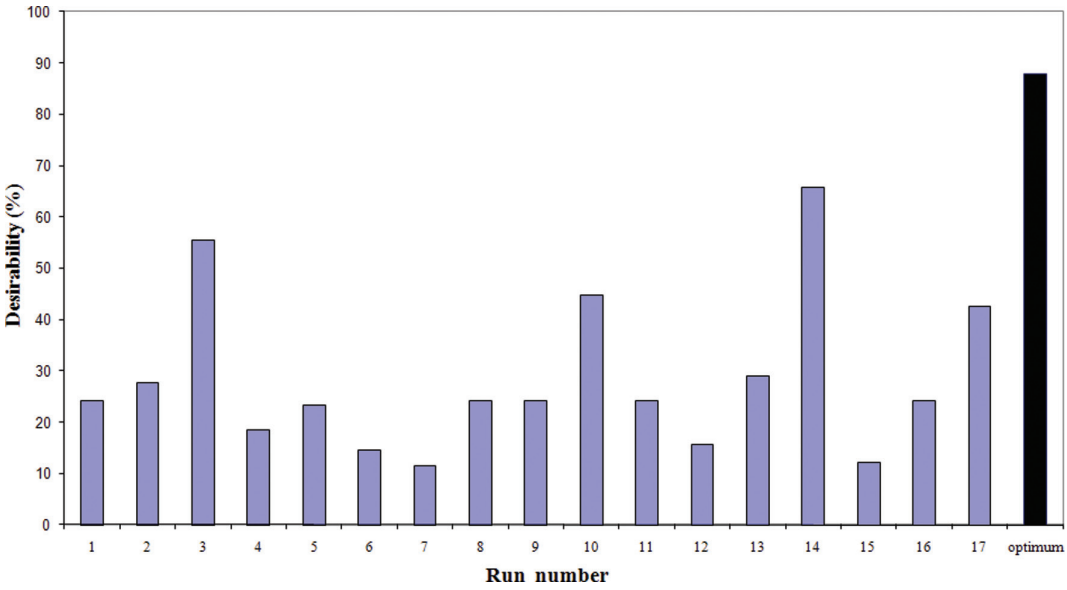

Fig. 12 Comparison between the desirability of second DOE runs and optimal working condition

5. The min–max optimization method allowed the identification of a parameter setting which gave the best compromise between the mutually contradictory QCs.
6. Producing a cylindrical cup with this parameter setting resulted in an optimal component. An additional advantage of this optimization approach is the flexibility with respect to customer requirements.
7. This approach allowed an examination of components with the selected sheet dimensions without the need to perform additional experiments. For new sheet dimensions, only a sub-set of the experiments would be required to be conducted.
8. The statistical methods described in this paper are easy to use and to implement. The proposed DOEs, ANOVA, and min–max optimization procedure is applicable to any forming process.

ACKNOWLEDGEMENT

The authors are grateful for the financial support provided through the UK ORSAS scheme.

REFERENCES

1 **Groche, P.** and **Schäfer, R.** Analysis of the geometrical tolerances and surface roughness of the spinning process. *Process scaling*, Volume 24, 2003 (BIAS, Bremen, Germany).

2 **El-Khabeery, M. M., Fattouh, M., El-Sheikh, M. N.,** and **Hamed, O. A.** On the conventional simple spinning of cylindrical aluminium cups. *Int. J. Mach. Tools Mf.*, 1991, **31**(2), 203–219.

3 **Quigley, E.** and **Monaghan, J.** The finite element modelling of conventional spinning using multi-domain models. *J. Mater. Process. Technol.*, 2002, **124**(3), 360–365.

4 **Quigley, E.** and **Monaghan, J.** Enhanced finite element models of metal spinning. *J. Mater. Process. Technol.*, 2002, **121**(1), 43–49.

5 **Zhan, M., Yang, H., Zhang, J. H., Xu, Y. L.,** and **Ma, F.** 3D FEM analysis of influence of roller feed rate on forming force and quality of cone spinning. *J. Mater. Process. Technol.*, 2007, **187–188**, 486–491.

6 **Wong, C. C., Dean, T. A.,** and **Lin, J.** Incremental forming of solid cylindrical components using flow forming principles. *J. Mater. Process. Technol.*, 2004, **153–154**, 60–66.

7 **Xia, Q., Shima, S., Kotera, H.,** and **Yasuhuku, D.** A study of the one-path deep drawing spinning of cups. *J. Mater. Process. Technol.*, 2005, **159**(3), 397–400.

8 **Liu, C.-H.** The simulation of the multi-pass and die-less spinning process. *J. Mater. Process. Technol.*, 2007, **192–193**, 518–524.

9 **Hamilton, S.** and **Long, H.** Analysis of conventional spinning process of a cylindrical part using finite element methods. *Steel Res. Int. J.*, 2008, **79**, 632–639.

10 **Bai, Q., Yang, H.,** and **Zhan, M.** Finite element modeling of power spinning of thin-walled shell with hoop inner rib. *Trans. Nonferr. Met. Soc. China*, 2008, **18**(1), 6–13.

11 **Behrouzi, A., Dariani, B. M.,** and **Shakeri, M.** Tool shape design in the sheet bending process by inverse analysis of springback. *Proc. IMechE, Part B: J. Engineering Manufacture*, 2009, **223**(10), 1331–1340. DOI: 10.1243/09544054JEM1561.

12 **Yang, C. L., Sheu, S. H.,** and **Yu, K. T.** Optimal machining parameters in the cutting process of glass fibre using the reliability analysis based on the Taguchi method. *Proc. IMechE, Part B: J. Engineering Manufacture*, 2008, **222**(9), 1075–1082. DOI: 10.1243/09544054JEM1134.

13 **Bacchewar, P., Singhal, S.,** and **Pandey, P.** Statistical modelling and optimization of surface roughness in the selective laser sintering process. *Proc. IMechE, Part B: J. Engineering Manufacture*, 2007, **221**(1), 35–52. DOI: 10.1243/09544054JEM670.

14 **Hussain, G., Gao, L.,** and **Hayat, N.** Empirical modelling of the influence of operating parameters on the spifability of a titanium sheet using response surface methodology. *Proc. IMechE, Part B: J. Engineering Manufacture*, 2009, **223**(1), 73–81. DOI: 10.1243/09544054JEM1259.

15 **Ham, M.** and **Jeswiet, J.** Forming limit curves in single point incremental forming. *CIRP Ann. - Mfg Technol.*, 2007, **56**(1), 277–280.

16 **Filice, L., Ambrogio, G.,** and **Micari, F.** On-line control of single point incremental forming operations through punch force monitoring. *CIRP Ann. - Mfg Technol.*, 2006, **55**(1), 245–248.

17 **Ham, M.** and **Jeswiet, J.** Single point incremental forming and the forming criteria for AA3003. *CIRP Ann. - Mfg Technol.*, 2006, **55**(1), 241–244.

18 **Ambrogio, G., Cozza, V., Filice, L.,** and **Micari, F.** An analytical model for improving precision in single point incremental forming. *J. Mater. Process. Technol.*, 2007, **191**(1–3), 92–95.

19 **Kleiner, M., Ewers, R., Kunert, J., Henkenjohann, N.,** and **Auer, C.** Optimisation of the shear forming process by means of multivariate statistical methods. Technical report 23/2005, SFB475. 2005, Universität Dortmund, Germany, 2005.

20 **Essa, K.** and **Hartley, P.** Numerical simulation of single and dual pass conventional spinning processes. *Int. J. Mater. Form.*, 2009, **2**, 271–281.

21 **Long, H.** and **Hamilton, S.** Simulation of effects of material deformation on thickness variation in conventional spinning. In Proceedings of the Ninth International Conference on *Technology of Plasticity*, Gyeongju, Korea, 7–11 September 2008.

22 **Kalpakjian, S.** and **Schmid, S.** *Manufacturing engineering and technology*, 2001 (Prentice Hall International, London, UK).

23 **Lange, K.** *Handbook of metal forming*. 1985 (SME publications, Dearborn, Michigan, USA).

24 **Lexian, H.** and **Dariani, B. M.** Effect of roller nose radius and release angle on the forming quality of a hot-spinning process using a non-linear finite element shell analysis. *Proc. IMechE, Part B: J. Engineering Manufacture*, 2009, **223**(6), 713–722. DOI: 10.1243/09544054JEM1445.

25 **Lind. D. A., Marchal. W. G.,** and **Wathen, S.** *Statistical techniques in business and economics*, 12th edition, 2005 (McGraw Hill Irwin, Boston, Massachusetts).